Effect Of Cracks On The Vibration And Bending Behavior Of Steel And Aluminum Bars Using Finite Element Analysis

Rajib Karmaker[1*], Md. Rashedul Islam[2], and Ujjwal Kumar Deb[3]

[1] Department of Mathematics, University of Chittagong , Chattogram, Bangladesh
[2] Department of Computer Science and Engineering, International Islamic University Chittagong, Chattogram, Bangladesh
[1,2,3] Department of Mathematics, Chittagong University of Engineering and Technology, Bangladesh
[*] Corresponding author. E-mail: rajibcumath@gmail.com

Received: May 14, 2023; Accepted: Aug. 25, 2023

Complex structures can develop cracks and defects over time, which can compromise their long-term performance and safety. Structural Health Monitoring (SHM) systems are essential for detecting and measuring these defects by monitoring the load and deformation of the solid materials. This paper presents a simulation study of the frequency and strength of solid cylindrical bars made of aluminum and steel under different loads and crack conditions. Finite Element Method (FEM) and COMSOL Multiphysics software are used to perform the simulation, and a resonance model is used to analyze the results. The study investigates how cracks affect the frequency and deformation of the bars, and how different materials respond to load and bending. The results show that frequency varies linearly with load, cracks decrease the stiffness and increase the frequency at the crack location, and aluminum bars deform more than steel bars. The paper concludes that steel bars are more resistant to load and bending than aluminum bars for both cracked and uncracked case. Finally, it is found that steel bars are more resistant to load and bending than aluminum bars for both cracked and uncracked case.

Keywords: Structural Health Monitoring, Load, Crack detection, Deflection, FEM.

http://dx.doi.org/10.6180/jase.202405_27(5).0011

1. Introduction

Structural Health Monitoring (SHM) is a growing research area that deals with the assessment of large and critical structures. These structures can suffer from various types of damage over time, which affect their local stiffness and flexibility [1]. SHM can provide reliable information about the structural integrity after extreme events such as earthquakes or heavy stress. The main benefit of SHM is that it can estimate the service life of structures and detect and locate structural anomalies. Cracks and deformation are common structural defects that cause local changes in stiffness and flexibility, which influence the dynamic behavior. In addition to cracks, another type of load-induced damage in structures is bending, which requires deflection analysis. The presence of cracks can be detected by using the differences in local stiffness, which have a significant impact on natural frequency and mode [2]. There are three types of vibration-based solution methods: analytical, numerical, and experimental [3]. Lee and Chung [4] proposed a new method to determine the first four natural frequencies of a cracked material using FEM, and to estimate the crack location using optimization. Later, Owolabi et al. [5] performed an experimental study on the effects of cracks and damages on the reliability of structures. Karmaker et al. [6] developed a computational approach using vibration analysis for the crack detection in structures such as beams. Various analytical, computational, and experimental methods are now used for crack detection in fiber-reinforced materials, laminated composites, and non-composite structures for vibrational analysis. In the same context, Goda et al. [7] used a simulation-based solution with finite elements to investigate the harmonic vibration response of fiber reinforced beams.

They used an eigenvalue analysis to perform dynamic modeling of the laminated beams, using an eight-node layered shell element to simulate vibrations. The main objective of their study was to assist mechanical designers in designing and developing composite structures subject to dynamic loadings. Rizos et al. [8] suggested a method for identifying crack location and depth by monitoring amplitudes at two different locations of a vibrating cantilever beam. They studied the flexural vibrations of a rectangular shaped beam structure with a longitudinal surface crack modeled as a rotational spring with low mass. They also assumed that the crack was fully open and constant in depth. They used a harmonic exciter to force the beam to vibrate at one of the natural modes of vibration and measured the amplitudes at two different locations in an experiment. The vibrational properties of a cracked Timoshenko beam were investigated by Kisa's research group [9]. In their study, FEM and component mode synthesis were used. The beam was divided into two parts and connected by a flexibility matrix that includes the interaction forces. The forces were derived from fracture mechanics expressions because the inversion of the stiffness matrix was done using stress intensity factors and strain energy release rate expressions.[10] developed a method for using a 1D FEA to locate structural damage in a beam. However, most studies have only focused on the effect of a single crack and undesirable behavior of various structural bodies. There is no effective mathematical model to detect the damages, evaluate the stability and behaviors of different materials. Therefore, this research aims to develop a mathematical model using the vibration analysis method to detect cracks, measure the deformation and frequencies in specific location of intact or cracked aluminum and steel bodies. The research also tries to analyze the complex behavior of simple crack systems in a systematic way. The Vibration Based Inspection (VBI) method is used as a potential tool for monitoring and identifying defects in machines and equipment. The Finite Element Method is used as the computational numerical method to provide detailed insights on crack models and stiffness matrices. The Euler- Bernoulli beam theory is used to describe the dynamic properties of beams with transverse cracks. The theoretical formulas for natural frequencies and mode shape for the bar are derived using appropriate boundary conditions due to the presence of a crack. The results are obtained numerically. The main advantage of this research is to provide a better interface for detecting hidden or explicit cracks in structural construction using minimum time and cost.

2. Numerical methods for computation

Computational numerical techniques are numerical methods that use computer programs to solve partial differential equations. Some common numerical methods for computation are- Finite Difference Method, Finite Volume Method, Boundary Element Method and Finite Element Method. The Finite Element Method (FEM) is the most widely used method for solving engineering and computational model problems. The FEM is a numerical method for solving partial differential equations with two or three variables in space [11]. FEA based simulations are valuable tools because they avoid the need for multiple physical prototype creation and testing for different high fidelity situations [12].

3. Mathematical model

To build analytical mathematical equations, we need to track some variables in a physical system. Some examples are mass conservation, energy efficiency, and force or power balance [13]. We can use this way of thinking to derive nonlinear systems for detecting any failure. We will see that many physical processes are modeled by the same partial differential equations, so we can develop and apply methods and theories for specific model problems to many different applications. We will also create a simulation process for the main steps of the non-destructive method of identifying three-dimensional fractures with different orientations in a uniform medium and detecting horizontal surface fractures, based on a unified bounding method. This includes the calculations of the load dissipation coefficient and deflection, and the generation of the asymptotic source field. We will use large aluminum and steel cylinders to study the frequencies and bending. The governing equations for deformation according to the Euler-Bernoulli Beam theory are,

$$EA\frac{d^2z}{dx^2} + p(x) = 0 \tag{1}$$

where, p(x) = cx = Applied load [c = constant] E = Young's Modulus A = Cross section area Z = Displacement

Subject to: $z(0) = 0$ and $\left|EA\frac{dz(x)}{dx}\right|_{x=L} = 0$

The release rate of strain energy at the cracked position is,

$$E_S = \frac{1}{E}\left(K_{I1} + K_{I2}\right)^2 \tag{2}$$

Where the stress concentration ratios of mode I (crack opening) are KI_1 and KI_2 under load P_1 and P_2 accordingly. $\frac{1}{\acute{E}} = \frac{1-\gamma_1^2}{E}$ (For plane strain condition), $\frac{1}{\acute{E}} = \frac{1}{E}$ (for plane stress condition)

Previous studies showed that, the expressions for stress distribution [13] are as follows:

$K_{I1} = \frac{P_1}{WH}\sqrt{\pi h\left(F_1\left(\frac{h}{H}\right)\right)}$ and $K_{I2} = \frac{6P_2}{WH^2}\sqrt{\pi h\left(F_2\left(\frac{h}{H}\right)\right)}$

Where parameters F_1 and F_2 can be presented as bellow,

$$F_1\left(\frac{h}{H}\right) = \sqrt{\frac{2H}{\pi h}\tan\left(\frac{\pi h}{2H}\right)} \times \left\{\frac{0.752 + 0.02\left(\frac{h}{H}\right) + 0.37\left(1 - \sin\left(\frac{\pi h}{2H}\right)\right)^3}{\cos\left(\frac{\pi h}{2H}\right)}\right\} \quad (3)$$

$$F_2\left(\frac{h}{H}\right) = \sqrt{\frac{2H}{\pi h}\tan\left(\frac{\pi h}{2H}\right)} \times \left\{\frac{0.923 + 0.199\left(1 - \sin\left(\frac{\pi h}{2H}\right)\right)^4}{\cos\left(\frac{\pi h}{2H}\right)}\right\} \quad (4)$$

The incremental movement along the direction of the applied force P_i according to Castiglione's theorem is,

$$z_i = \frac{\delta U_c}{\delta P_i} \quad (5)$$

Where U_c = strain energy, so that $z_i = \frac{\delta}{\delta P_i}\left[\int_0^{h_1} J_c(h)dh\right]$ where $J_c = \frac{\delta U_c}{\delta h}$ = strain energy release rate.

Estimating the C_{ij} per unit thickness adaptability effect co-efficient,

$$C_{ij} = \frac{\delta z_i}{\delta P_i} = \frac{\delta^2}{\delta P_i \delta P_j}\left[\int_{-W/2}^{W/2}\int_0^{h_1} J_c(h)dhdz\right] \quad (6)$$

With the strain energy release rate,

$$C_{ij} = \frac{B}{E}\frac{\delta^2}{\delta P_i \delta P_j}\left[\int_0^{h_1}(K_{I1} + K_{I2})\, dh\right] \quad (7)$$

The stiffness matrix becomes,

$$K = \begin{bmatrix} K_{11} & K_{12} \\ K_{21} & K_{22} \end{bmatrix} \times \begin{bmatrix} C_{11} & C_{12} \\ C_{21} & C_{22} \end{bmatrix}^{-1} \quad (8)$$

4. Geometry and mesh statistics

Fig. 1 depicts solid tubular shaped steel and aluminum bar with length 0.15 m and radius is 0.015 m, crack depth (D) and initial crack length (cl) are 0.003 m and 0.00033 m respectively. Fig. 2 shows the mesh design of considered domain for intact and cracked aluminum and steel bar.

Table 1 exhibit the mesh properties of the computational domain and Table 2 show the characteristics of the simulation.

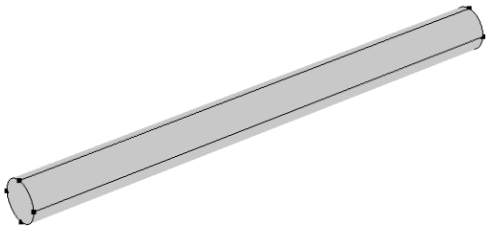

Fig. 1. Computational domain with crack

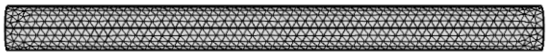

(a) Mesh of uncracked bar

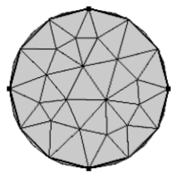

(b) Mesh of inlet cross section

Fig. 2. Mesh design

5. Results and discussions

Using the Finite Element Method, the frequencies of steel and aluminum bars with semicircular twin cracks were computed. Solid cylindrical bars of steel and aluminum were modeled with COMSOL Multiphysics simulation software [14] and various parameters from COMSOL Multiphysics, which are listed in Tables 3 and 4 respectively, were applied.

The vertical loads applied to the apex of the bar are shown in Fig. 3 and the resulting deformation of the body is shown in Fig. 4. The dynamic properties and deflection of bars were determined using Euler-Bernoulli beam theory.

Fig. 5 shows how the load is distributed throughout the computational domain. Neither steel nor aluminum bars have cracks, as seen in Fig. 5 [(a)-(b)]. The stress is

Fig. 3. Load on apex of the domain

Table 1. Mesh statistics of the domain

Particulars	Value	Particulars	Value
Element quality(min)	0.1315 mm	Element size(min)	0.022 mm
Element quality (Average)	0.6792 mm	Element size(max)	0.0016 mm
Tetrahedron elements	17413	Curvature factor	0.4
Triangle elements	4182	Regional resolution	0.7
Edge elements	517	Growth rate of element	1.4
Vertex elements	20	Predefined shape	Finer

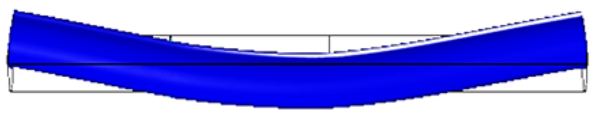

Fig. 4. Deformation after applying load

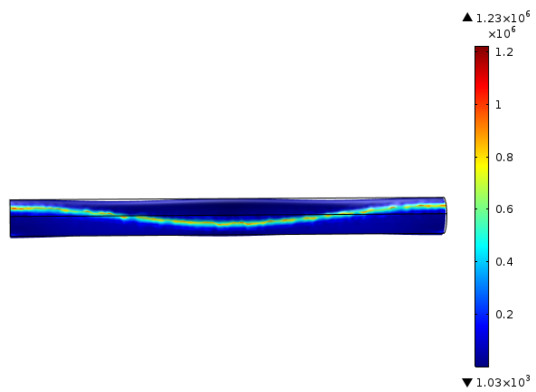

(a) Uncracked Steel

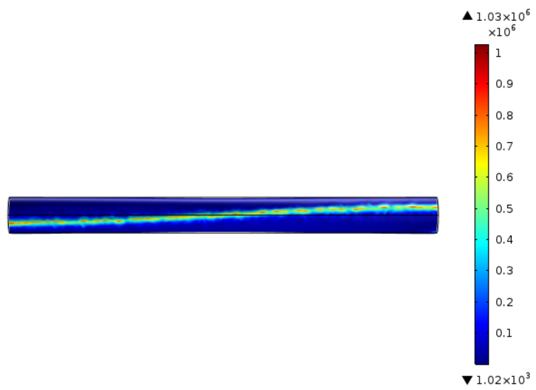

(b) Uncracked Aluminum

Fig. 5. Phase of load distribution in uncracked body

Table 2. Characteristics of simulation

Particulars	Value
Degrees of freedom	17687
Domain	1
Dimension	3
Edge elements	485
Boundaries	15
Boundary elements	3976
Strain reference temperature	293.17 K

Table 3. Geometry of the domain

Particulars	Value
Crack's width (cl)	0.00033 m
Crack's depth (ch)	0.03 m
Length of domain(L)	0.15 m
Radius of domain (r)	0.015 m

absorbed and spread evenly to the ends of the body by both bars. Aluminum has more deflection than steel, as observed.

Fig. 6 shows how the load is absorbed at each fracture point. The load is distributed evenly to the ends of the fatigue point in steel. Aluminum behaves similarly to steel, but it does not distribute the force as uniformly throughout the whole body as steel does.

The slice of load concentration at crack locations is shown in Fig. 7. The load is highest at the bottom, as observed. It is also noted that the load was applied at the apex and reached the lower part with strong vibration and variable frequency, especially at the cracked point.

The fluctuations in frequencies at different positions are more significant for cracked bars than uncracked ones, as shown in Fig. 8. The frequencies are also highest at the cracked positions. The line graph is mostly normal, even at the relevant fracture point in the upper part of the steel bar. Aluminum shows a fairly regular line graph for its flexibility variation. This means that the maximum frequency is transmitted to the closest area.

Table 4. Properties of Materials

Particulars	Steel	Aluminum	Unit
Young's modulus	201	115	GPa
Density	7850	2700	kg/m^3
Poisson's ratio	0.30	0.36	1
Shear modulus	73.3e9	35.7e9	N/m^2
Tensile Strength	430	240	MPa
Relative permeability	1	1.0001	1
Thermal conductivity	44.5	24.5	$W/(m * K)$

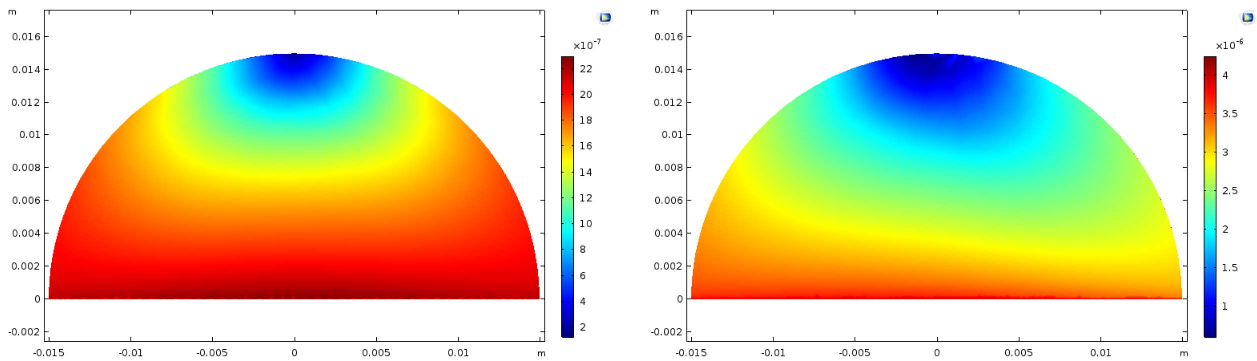

(a) (b)

Fig. 6. Load distribution at cracked points

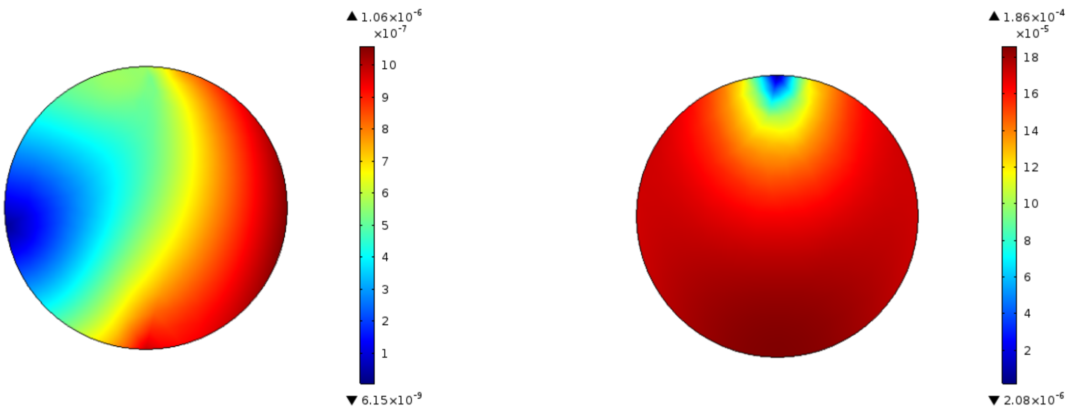

(a) (b)

Fig. 7. Reserved loads near the cracks

The line graph also shows a considerable difference for uneven load distribution. The load in steel and aluminum structures is distributed throughout the whole body, but this distribution is more uniform in steel than aluminum.

The Fig. 9 shows that the frequencies for both bodies increase with the increase of load. It is observed that an inconsistent behavior where one fracture took more load than the others after applying load. The total frequency of an aluminum bar under different loads is higher than that of a steel body at a fracture point, because the frequencies increase proportionally to the stress distribution. Therefore, it can be noted that the aluminum body has a higher risk of damage than the steel body when we apply load to a fatigue body.

The deformation line graph is almost the same for both bodies, as seen in Fig. 10. The graphs have regular fluctuations but no major disruptions in the curve. The bending in

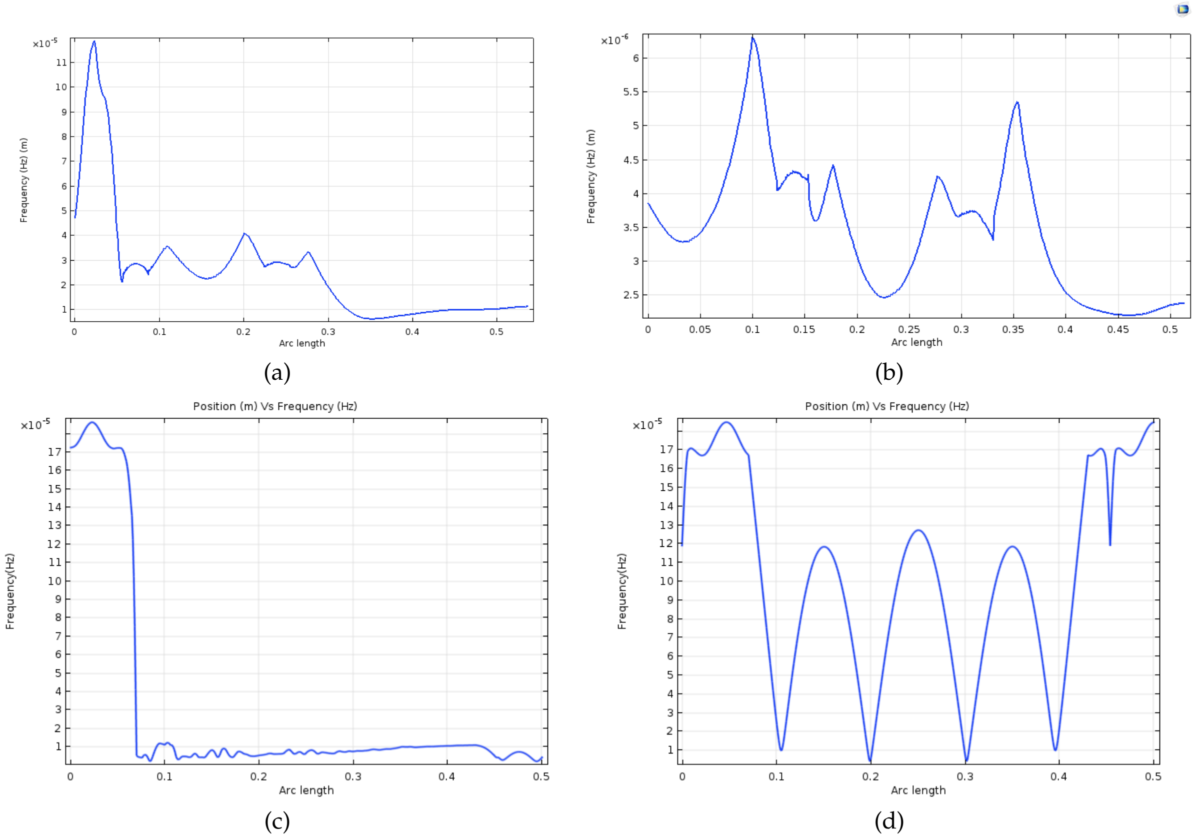

Fig. 8. Line graphs of frequency

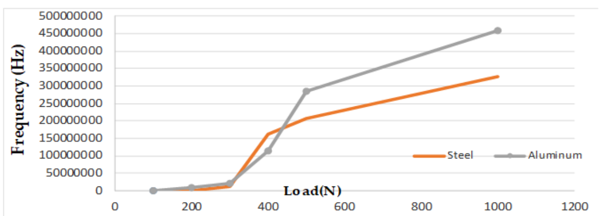

Fig. 9. Different applied load vs frequency

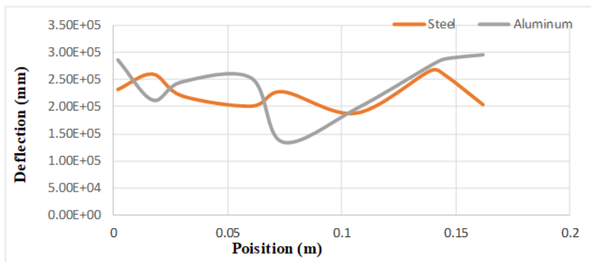

Fig. 10. Line graph of deformation of uncracked bodies

cracked bodies is shown in Fig. 11. The line graphs show that the aluminum bar has more deformation due to load than the steel body. This is true for both cracked and uncracked situations. It is also seen that the deformation is higher at the cracked positions.

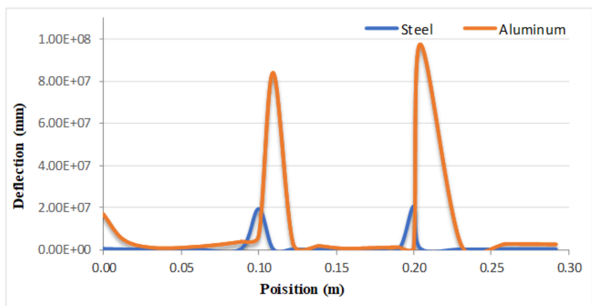

Fig. 11. Line graph of deformation of cracked bodies

5.1. Discussion

Compared to aluminum bars, steel bars showed greater resistance to load and bending, as they could share the load equally and cope with different amounts of stress and vibration. Aluminum bars, in contrast, kept the stress at the crack site and twisted and shook more due to their lighter weight and higher flexibility. This could endanger the structural quality or performance. Hence, steel bars are more desirable than aluminum bars for their toughness, versatility, and dependability. The FEA results are confirmed by matching them with experimental data from Khan et al. [15] and a good correlation was seen.

6. Conclusion

This study applied the Finite Element Method to simulate the frequency and deflection of steel and aluminum bars with two transverse cracks under different loads. The cracks created new boundary conditions for the structures, which reduced the natural frequencies and modified the mode shapes of vibrations. A method was developed to predict the location and deflection of a crack in a steel and aluminum bar using vibrational data, and to investigate the mode shape bending characteristics of a composite bar with a longitudinal open crack subject to free vibration. The results showed that the frequency susceptibility of cylindrical shape steel and aluminum bars changed with crack location for all vibration modes. The results also showed that steel bars were more resistant to load and bending than aluminum bars, as they could distribute the applied weight uniformly throughout the structure and absorb varied amounts of stress and induced vibration. Aluminum bars, on the other hand, reserved the stress at any one point, causing excessive vibration and deflection in the affected region of the structure, which could lead to damage or distortion. Moreover, aluminum is a light metal that may not be suitable for large construction. Therefore, this study suggests that steel bars may be more acceptable and advantageous than aluminum bars for structural health monitoring systems design and optimization, due to their strong corrosion resistance, elasticity, and diverting capacity.

Acknowledgement

The authors gratefully acknowledge for the technical support to The Centre of excellence in Mathematics, Department of Mathematics, Mahidol University, Bangkok, Thailand.

References

[1] A. Priyadarshini. *"Identification of Cracks in Beams using Vibrational Analysis"*. (mathesis). National Institute of Technology, Rourkela-769008, 2013.

[2] L. Rubio, (2009) *"An Efficient Method for Crack Identification in Simply Supported Euler–Bernoulli Beams"* **ASME Journal of Vibration and Acoustics *131***: 051001–6. DOI: 10.1115/1.3142876.

[3] S. Taylor and D. Zimmerman, (2010) *"Improved Experimental Ritz Vector Extraction with Application to Damage Detection"* **ASME Journal of Vibration and Acoustics *132***: 011010–12. DOI: 10.1115/1.4000762.

[4] M. S. Young and J. Chung, (2000) *"A study on crack detection using eigen frequency test data"* **Journal of Computers and Structures *77***: 327–342.

[5] G. Owolabi, A. Swamidas, and R. Seshadri, (2003) *"Crack detection in beams using changes in frequencies and amplitudes of frequency response functions"* **Journal of Sound and Vibration *265***: 1–22. DOI: 10.1016/S0022-460X(02)01264-6.

[6] R. Karmaker, U. Deb, and A. Das, (2020) *"Modeling and Simulation of a Cracked Beam with Different Location Using FEM"* **Computational Water, Energy, and Environmental Engineering *9***: 145–158.

[7] I. Goda, J. Ganghoffer, and M. Aly. "Parametric Study on the Free Vibration Response of Laminated Composite Beams". In: *Mechanics of Nano, Micro and Macro Composite Structures*. Politecnico di Torino, 2012, 18–20.

[8] R. Rizos, N. Aspragathos, and A. Dimarogonas, (1990) *"Identification of crack location and magnitude in a cantilever beam from the vibration modes"* **Journal of Sound and Vibration *138***(3): 381–388. DOI: 10.1016/0022-460X(90)90593-O.

[9] M. Kisa, J. Brandon, and M. Topcu, (1998) *"Free vibration analysis of cracked beams by a combination of finite elements and component mode synthesis methods"* **Journal of Computers and Structures *67***: 215–223. DOI: 10.1016/S0045-7949(98)00056-X.

[10] C. Ratcliffe, (1997) *"Damage detection using a modified Laplacian operator on mode shape data"* **Journal of Sound and Vibration *204***(3): 505–517. DOI: 10.1006/jsvi.1997.0961.

[11] A. Dimarogonas, (1996) *"Vibration of cracked structures: a state of the art review"* **Engineering Fracture Mechanics *55***(5): 831–857. DOI: 10.1016/0013-7944(94)00175-8.

[12] A. Shukla, A. Singh, and P. Singh, (2011) *"A Comparative Study of Finite Volume Method and Finite Difference Method for Convection-Diffusion Problem"* **American Journal of Computational and Applied Mathematics *1***(2): 67–73.

[13] G. Irwin, (1956) *"Analysis of stresses and strains near the end of a crack transverse in a plate"* **Journal of Applied Mechanics *24***: 361–364.

[14] *COMSOL Multiphysics*. COMSOL Inc. 2021.

[15] M. Khan, K. Akhtar, N. Ahmad, et al., (2020) *"Vibration analysis of damaged and undamaged steel structure systems: cantilever column and frame"* **Earthquake Engineering and Engineering Vibration *19***: 725–737. DOI: 10.1007/s11803-020-0591-9.